Charm Lifetimes, $D^0 - \overline{D}^0$ Mixing and Double $c\bar{c}$ Continuum Production

Pavel Pakhlov
Institute of Theoretical and Experimental Physics
117259 Moscow, RUSSIA

1 Charm Lifetimes

The study of charm hadron lifetimes, which span one order of magnitude, is essential for understanding of strong interactions. Improved precision of the charm lifetimes measurements stimulates the development of theoretical models which are now able to explain quantatively the observed lifetime hierarchy.

The FOCUS Collaboration presents the most accurate measurement of the lifetime of D^0 and D^+ mesons using the samples of $\sim$140,000 $D^0 \to K^-\pi^+$, $\sim$68,000 $D^0 \to K^-\pi^+\pi^+\pi^-$, and $\sim$110,000 $D^+ \to K^-\pi^+\pi^+$ candidates. A lifetime fit is performed to the proper time distribution in the signal region. The proper time is extracted from the distance between the primary and secondary vertices. The vertexing algorithm is found to provide very uniform proper time acceptance. The measured lifetimes are $409.6 \pm 1.1 \pm 1.5$ fs for D^0 and $1039.4 \pm 4.3 \pm 7.0$ fs for D^+, where the first error is statistical and the second is systematic. The details of this analysis can be found in Ref. [1]. These results are in good agreement with the measurements of other experiments [2, 3] but surpass them in accuracy by a factor of $2-3$.

2 $D^0 - \overline{D}^0$ Mixing

In presence of $D^0 \leftrightarrow \overline{D}^0$ transitions the flavour eigenstates are different from the mass eigenstates, characterized by a mass splitting (Δm) and a width difference ($\Delta\Gamma$). Two different mechanisms which are responsible for $D^0 - \overline{D}^0$ mixing (quark box diagrams and long-distance hadronic interations) are suppressed by GIM mechanism and $SU(3)_{\rm FL}$ symmetry. The $D^0 - \overline{D^0}$ mixing parameters defined as $x = \Delta m/\Gamma$ and $y = \Delta\Gamma/2\Gamma$ are predicted to be smaller than 10^{-3} in the SM. However x can be significantly enhanced by non-SM processes while final state interactions and $SU(3)_{\rm FL}$-breaking can encance y to a level achievable by the current experimental sensitivity.

The FOCUS measurement [4] of y_{CP} (which is, in the CP-conserving limit, equal to y) of $(3.42 \pm 1.39 \pm 0.74)\%$ has aroused additional interest in $D^0 - \overline{D}^0$ mixing. More recent experimental measurements by the CLEO and Belle Collaborations [5, 3]

have not confirmed, though they have not completely refuted, the large FOCUS y_{CP} value. Recently the BaBar Collaboration has performed a new measurement of the parameter y_{CP} based on a data sample of $57.8\,\mathrm{fb}^{-1}$ collected with the BaBar detector, at the PEP-II asymmetric e^+e^- collider. D^0 candidates, reconstructed in $K\pi$, KK and $\pi\pi$ decay modes, are required to be produced in $D^{*+} \to D^0\pi^+$ decay. This provides samples of unsurpassed purity. Finally $158,000$ $D^0 \to K\pi$, $16,500$ $D^0 \to KK$, and $8,350$ $D^0 \to \pi\pi$ candidates with signal purities of about 99.5%, 97.1% and 92.4% respectively are selected within the D^0 signal region. The D^0 proper time is derived, in the plane transverse to the beam direction, from the flight length defined as the distance between the D^0 and D^{*+} vertices projected on the D^0 transverse momentum. An unbinned maximum likelihood fit is used to extract the lifetime for the three D^0 samples. The results of the fits are shown in Figure 1 superimposed on the proper time distributions for the three decay modes.

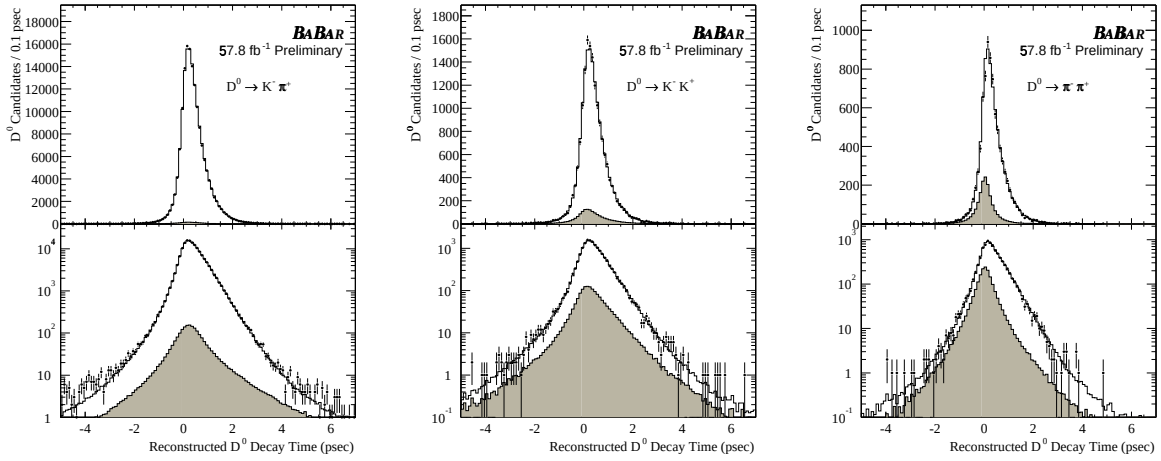

Figure 1: The open histogram represents the result of the unbinned maximum likelihood fit; the shaded one is the portion assigned to the background by the fit.

The measured values of y_{CP} for the KK and $\pi\pi$ modes are equal to $(1.5\pm1.3^{+0.6}_{-0.7})\%$ and $(1.0\pm1.7^{+1.2}_{-1.4})\%$ respectively. Their average of $y_{CP} = (1.4\pm1.0^{+0.6}_{-0.7})\%$ is consistent with zero but suggests a positive value not incompatible with the FOCUS result.

3 Double $c\bar{c}$ Continuum Production

Prompt charmonium production in e^+e^- annihilation provides an opportunity to study both perturbative and non-perturbative effects in QCD. The NRQCD [6, 7, 8, 9] model predicts that prompt J/ψ production at $\sqrt{s} \approx 10.6\,\mathrm{GeV}$ is dominated by $e^+e^- \to J/\psi\, gg$, with additional contributions from $J/\psi\, g$, $J/\psi\, c\bar{c}$ and other processes. Both BaBar and Belle Collaborations [10] presented cross-section measurements for

prompt J/ψ and $\psi(2S)$ production, and studies of their kinematic properties, which were compared to predictions of the models. However, these results do not constrain the contributions from particular mechanisms.

The Belle Collaboration presents the results of a search for $J/\psi\, c\bar{c}$ production, *i.e.* double $c\bar{c}$ production, where the additional $c\bar{c}$ pair fragments into either charmonium or charmed hadrons. The analysis is based on $46.2\,\mathrm{fb}^{-1}$ of data, collected at the $\Upsilon(4S)$ and nearby continuum with the Belle detector at the KEKB asymmetric energy storage rings. The details of event selection and J/ψ reconstruction can be found in Ref. [11].

Distributions of the mass of the system recoiling against the J/ψ candidate—the "recoil mass"—are shown in Fig. 2*a*, for both J/ψ signal and sideband regions. The recoil mass is defined as $M_{\mathrm{recoil}} = \sqrt{(E_{CMS} - E_{J/\psi})^2 - p^2_{J/\psi}}$. A clear threshold near $2\,m_c$ can be seen for the J/ψ signal region. The region $2\,m_c < M_{\mathrm{recoil}} < 2\,m_D$ is studied

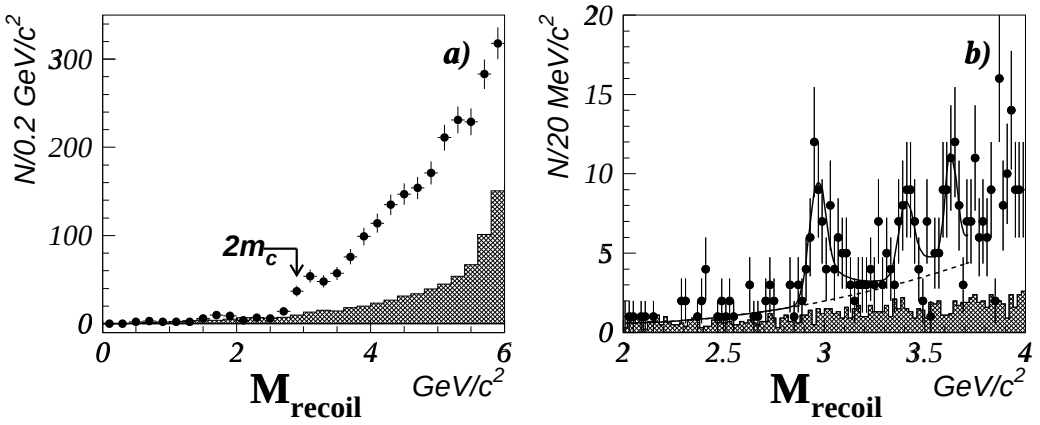

Figure 2: a) The recoil mass distribution for the J/ψ signal region (points) and scaled sidebands (hatched histogram). b) The recoil mass distribution after refitting the J/ψ candidate with a mass constraint for the J/ψ signal region (points) and scaled sidebands (hatched histogram). The curve represents the fit.

in more detail in order to search for production of J/ψ together with an additional charmonium state. A mass constrained fit is applied to the J/ψ candidates before determining $p_{J/\psi}$ to improve the M_{recoil} resolution. The resulting recoil mass spectrum in the data is presented in Fig. 2*b*: a clear peak is observed around $3\,\mathrm{GeV}/c^2$ which can be interpreted as $e^+e^- \to J/\psi\,\eta_c$. Additional peaks at recoil masses consistent with the χ_{c0} and $\eta_c(2S)$ mass are also seen. The fit procedure is described in detail in Ref. [11] and the fit results are presented in Table 1. To determine the $e^+e^- \to J/\psi\,\eta_c(\gamma)$ cross-section the signal yield is corrected for the reconstruction efficiency obtained from the Monte Carlo. Because of the selection requirement that the total charged multiplicity in the event be greater than 4, the recoil system must contain

at least three charged tracks: this removes η_c decays into 0 or 2 charged tracks plus neutrals. As η_c branching fractions are poorly known, the result is expressed in terms of the product $\sigma(e^+e^- \to J/\psi\,\eta_c\,(\gamma)) \times \mathcal{B}(\eta_c \to \geq 4\,\text{charged})$, and found to be $(0.033\,^{+0.007}_{-0.006} \pm 0.009)$ pb.

To study the $J/\psi\,c\overline{c}$ mechanism in the region $M_{\text{recoil}} \geq 2\,m_D$, a search is performed for fully reconstructed D^{*+} and D^0 decays in events with a J/ψ meson. Real $J/\psi D$ combinations from $B\overline{B}$ decays are totally discarded by the event selection using the kinematical properties of $B\overline{B}$ events. For selected $J/\psi D^{*+}$ candidates the scatter plot of the dilepton mass versus the $D^0\pi^+$ mass, and the $D^0\pi^+$ mass projection, are shown in Figs. $3a,b$. The signal yield, found from a simultaneous fit to the $D^0\pi^+$ mass distributions for J/ψ signal and sideband windows, is equal to $N_{J/\psi\,D^{*+}} = 10.1^{+3.6}_{-3.0}$, with significance $\sigma_{J/\psi\,D^{*+}} = 5.3$. A plot of dilepton versus $K^-\pi^+(K^-K^+)$ masses,

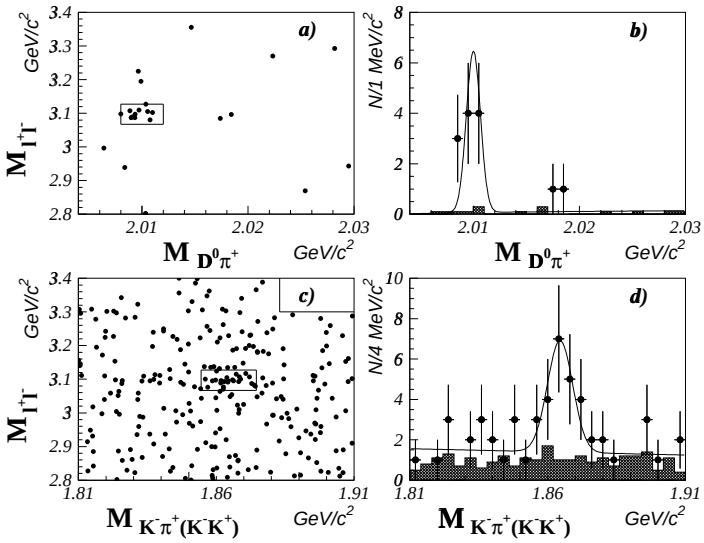

Figure 3: Results of a search for associated production of J/ψ and charm mesons: a) the scatter plot $M(l^+l^-)$ vs $M(D^0\pi^+)$; b) projection onto the $M(D^0\pi^+)$ axis; c) the scatter plot $M(l^+l^-)$ vs $M(K^-\pi^+(K^+K^-))$; d) projection onto the $M(K^-\pi^+(K^+K^-))$ axis. Points with error bars show the J/ψ signal region and the hatched histograms show the scaled sidebands. The curves represent the fit.

	N	$M\,[\text{GeV}/c^2]$	σ
$J/\psi\,\eta_c$	67^{+13}_{-12}	2.962 ± 0.013	6.7
$J/\psi\,\chi_{c0}$	39^{+14}_{-13}	3.403 ± 0.014	3.3
$J/\psi\,\eta_c(2S)$	42^{+15}_{-13}	3.622 ± 0.012	3.4

Table 1: The results of the fit to the recoil mass distribution.

and the projection onto the $K^-\pi^+(K^-K^+)$ mass axis, are shown in Figs. 3*c,d*. A simultaneous fit to the $K^-\pi^+$ (K^-K^+) mass distribution in the J/ψ signal window and the sideband finds $N_{J/\psi\,D^0} = 14.9^{+5.4}_{-4.8}$, with significance $\sigma_{J/\psi\,D^0} = 3.7$. Correcting for the efficiencies found by the Monte Carlo simulation, the cross-sections of $e^+e^- \to J/\psi\,D^{*+}\,X$ and $e^+e^- \to J/\psi\,D^0\,X$ are found to be $(0.53\,^{+0.19}_{-0.15} \pm 0.14)$ pb and $(0.87\,^{+0.32}_{-0.28} \pm 0.20)$ pb respectively. From these values the $e^+e^- \to J/\psi\,c\bar{c}$ cross-section can be derived in model-dependent way, using the model predictions for $c\bar{c}$ fragmentation rates into D^{*+} and D^0. Using the Lund model and averaging over two results the $e^+e^- \to J/\psi\,c\bar{c}$ cross-section is calculated to be $(0.87\,^{+0.21}_{-0.19} \pm 0.17)$ pb. This $J/\psi\,c\bar{c}$ cross-section is an order of magnitude larger than predicted in Refs. [7, 9, 12], and contradicts the NRQCD expectation that the $J/\psi\,c\bar{c}$ fraction is small [7, 9].

References

[1] J.M. Link *et al.* (FOCUS Collab.), Phys. Lett. **B537**, 192 (2002).

[2] P.L. Frabetti *et al.* (E687 Collab.), Phys. Lett. **B323**, 459 (1994); G. Bonvicini *et al.* (CLEO Collab.), Phys. Rev. Lett. **82**, 4586 (1999); E.M. Aitala *et al.* (E791 Collab.), Phys. Rev. Lett. **83**, 32 (1999).

[3] K. Abe *et al.* (Belle Collab.), Phys. Rev. Lett. **88**, 162001 (2002).

[4] J. M. Link *et al.* (FOCUS Collab.), Phys. Lett. **B485**, 62 (2000).

[5] S. E. Csorna *et al.* (CLEO Collab.), Phys. Rev. **D65**, 092001 (2002)

[6] E. Braaten and S. Fleming, Phys. Rev. Lett. **74**, 3327 (1995); P. Cho and M. Wise, Phys. Lett. **B346**, 129 (1995); M. Cacciari, M. Greco, M. L. Mangano, and A. Petrelli, *ibid.* **B356**, 553 (1995).

[7] P. Cho and A. K. Leibovich, Phys. Rev. D **53**, 150 (1996); **53**, 6203 (1996). S. Baek, P. Ko, J. Lee, and H. S. Song, J. Kor. Phys. Soc. **33**, 97 (1998).

[8] E. Braaten and Yu-Qi Chen, Phys. Rev. Lett. **76**, 730 (1996).

[9] F. Yuan, C.-F. Qiao, and K.-T. Chao, Phys. Rev. D **56**, 321 (1997).

[10] B. Aubert *et al.* (BaBar Collab.), Phys. Rev. Lett. **87** 162002 (2001); K. Abe *et al.* (Belle Collab.), Phys. Rev. Lett. **88**, 052001 (2002).

[11] K. Abe *et al.* (Belle Collab.), hep-ex/0205104, Submitted to Phys. Rev. Lett.

[12] V. V. Kiselev, A. K. Likhoded, and M. V. Shevlyagin, Phys. Lett. **B332**, 411 (1994).